Gas-Phase Infrared and ab Initio Study of the Unstable CF_3CNO Molecule and Its Stable Furoxan Ring Dimer

Balázs Havasi,[†] Tibor Pasinszki,*[,†] and Nicholas P. C. Westwood*[,‡]

Department of Inorganic Chemistry, Budapest University of Technology and Economics, H-1521 Budapest, Gellért tér 4, Hungary, and Guelph-Waterloo Centre for Graduate Work in Chemistry, Department of Chemistry, University of Guelph, Guelph, Ontario, Canada N1G 2W1

Received: November 19, 2004

The unstable trifluoroacetonitrile *N*-oxide molecule, CF_3CNO, has been generated in high yield in the gas phase from $CF_3BrC{=}NOH$ and studied for the first time by gas-phase mid-infrared spectroscopy. Cold trapping of this molecule followed by slow warming forms the stable ring dimer, bis(trifluoromethyl)furoxan, also investigated by gas-phase infrared spectroscopy. The spectroscopy provides an investigation into the vibrational character of the two molecules, the assignments supported by calculations of the harmonic vibrational frequencies using in the case of CF_3CNO both ab initio (CCSD(T)) and density functional theory (B3LYP) and B3LYP for the ring dimer. The ground-state structures of both molecules were investigated at the B3LYP level of theory, with CF_3CNO further investigated using coupled-cluster. The CCSD(T) method suggests a slightly bent (C_s) structure for CF_3CNO, while the B3LYP method (with basis sets ranging from 6-311G(d) to cc-pVTZ) suggests a close-to-linear or linear CCNO chain. The CCN bending potential in CF_3CNO was explored at the CCSD(T)(fc)/cc-pVTZ level, with the results suggesting that CF_3CNO exhibits strong quasi-symmetric top behavior with a barrier to linearity of 174 cm^{-1}. Since both isomerization and dimerization are feasible loss processes for this unstable molecule, the relative stability of CF_3CNO with respect to the known cyanate (CF_3OCN), isocyanate (CF_3NCO), and fulminate (CF_3ONC) isomers and the mechanism of the dimerization process to the ring furoxan and other isomers were studied with density functional theory.

Introduction

Small nitrile oxides, archetypal 1,3-dipolarophiles, are short-lived reactive intermediates, difficult to produce and observe in the free state. Nonetheless, they are widely used in organic chemistry for the syntheses of heterocycles and natural products,[1−5] mainly by in situ preparation and subsequent 1,3-dipolar reaction with various substrates. Trifluoroacetonitrile *N*-oxide, CF_3CNO (**1**), is often used in [2 + 3] cycloaddition reactions where five-membered heterocycles, for example, oxazoles, oxazolines, isoxazoles, and isoxazolines, including Diels−Alder adducts, can be prepared.[6−12] Recently, **1** has proven to be of interest in medical applications, acting as a reagent for preparing tachykinin receptor antagonists[13] as well as in the production of herbicides, pesticides, and insecticides.[14] In most cases, **1** is generated as a reactive dipolarophile in solution from Br- or Cl-oximes, specifically trifluoroacetohydroximoyl bromide and chloride, respectively, since it has been stated[6] to be unstable in solution "even at a temperature below −20°".

The structural and spectroscopic properties of the unstable CF_3CNO molecule have, hitherto, not been investigated experimentally but, nevertheless, are of interest because of issues arising from the linearity or nonlinearity of the CCNO frame. Recent experimental work has demonstrated a propensity for simple nitrile oxide molecules (XCNO, X=Br,[15,16] NC,[17,18] Cl[16,19]) to exhibit quasi-linear behavior with the precise bending potential strongly dependent on the nature of the substituent, X. Hence, ClCNO and BrCNO have been described as "extremely quasi-linear",[16] whereas "it is a matter of taste"[18] if NCCNO is linear or quasi-linear. On the other hand, with a strong electron withdrawing group (X=F), FCNO (never observed experimentally) is predicted by ab initio and density functional theory (DFT) methods to be bent.[20,21] An important issue for the present work is whether the strongly electron withdrawing CF_3 group in **1** leads to a bent CCN structure (C_s) or, by analogy with the structure of acetonitrile *N*-oxide, CH_3CNO,[22] the trifluoro-analogue (**1**) is a symmetric top (C_{3v}). Previous computational studies are limited; ab initio (HF/4-31G*)[23] and semiempirical (MNDO)[24] calculations suggest a linear CCNO framework.

Nitrile oxides are known to dimerize via cycloaddition to furoxans (1,2,5-oxadiazole-2-oxides),[1−5] and so the generation of **1** provides the opportunity to investigate, following condensation, the formation of bis(trifluoromethyl)furoxan (**2**), the known ring dimer of CF_3CNO. **2** has been previously prepared by the reaction of 2,2,2-trifluorodiazoethane and N_2O_4[25] and from the reaction of trifluoroacetohydroximoyl chloride and NaOH.[12] The only known gas-phase study is that by mass spectroscopy, giving the characteristic large fragment peak at $m/z = 30$ (NO^+).[26] Furoxans have spawned recent interest not only because of their synthetic utility for preparing pharmacologically and agrochemically active agents[27] but also because of their potential as NO generators, as biological messengers,[28] and as sources of high-density energetic materials of use as explosives. Investigation of the thermolytic cleavage of aryl/alkyl-[29,30] and cyanofuroxans,[31] successfully used for the spectroscopic investigation of the unstable CH_3CNO[22] and

* To whom correspondence should be addressed. E-mail: pasinszki@mail.bme.hu (T.P.); westwood@uoguelph.ca (N.P.C.W.).
[†] Budapest University of Technology and Economics.
[‡] University of Guelph.

10.1021/jp040725f CCC: $30.25
Published on Web 04/08/2005

$NCCNO$[17] molecules, suggests a similar opportunity to investigate the thermolysis of **2**.

In this work, we report the gas-phase generation of **1** and its stable furoxan dimer (**2**) and an investigation of their vibrational properties and geometric structures by mid-infrared (IR) spectroscopy and ab initio/DFT calculations. Of particular interest are the generation of the molecules, the structure of the nitrile oxide (linear, quasi-linear, or bent CCNO frame), its stability and potential conversion processes involving isocyanate, cyanate, fulminate and related isomers, and dimerization mechanisms to the furoxan and related dimers.

Experimental Section

Trifluoroacetohydroximoyl bromide ($CF_3BrC{=}NOH$) was chosen as a potential precursor for the generation of **1**. The preparation of this oxime by multistep synthesis has been described in detail.[8] Reduction of CF_3COOH (Aldrich) with $LiAlH_4$ (Aldrich) in diethyl ether gave $CF_3CH(OH)_2$. This species reacts with $NH_2OH{\cdot}HCl$ (Aldrich) in ether to provide $CF_3CH{=}NOH$ as an etherate complex which was brominated to the desired product, $CF_3BrC{=}NOH{\cdot}Et_2O$, using NBS (*N*-bromosuccinimide, Aldrich). Sample purity was confirmed by gas-phase IR.

Four methods (described in the Results and Discussion section), based on the $CF_3BrC{=}NOH{\cdot}Et_2O$ precursor, were used to generate **1** in a flow system for gas-phase IR measurement. On-line condensation of **1** at low temperature in a U-trap and its subsequent dimerization upon warming was used to produce **2**, to assess the ability of **1** to revaporize, and as a source of **2** for IR and thermolysis experiments.

IR spectra (resolution 0.5 cm^{-1}) were collected on a Nicolet Nexus 870 using a flow-through, single-pass (20 cm) cell and a room-temperature DTGS detector. The cell, with KBr windows, gave a spectral range from 4000 to 400 cm^{-1}. The gaseous effluent from the reaction tube was pumped either directly or via U-traps through the cell using an Edwards E2M5 rotary pump. Spectra were obtained at pressures between 300 and 1000 mTorr.

Computational Methods

Preliminary calculations for the structure of **1** suggested a very flat potential for CCN bending, and so the structure of the molecule and any barrier to linearity were calculated with both DFT and ab initio methods with a range of basis sets. DFT calculations were carried out at the B3LYP level using basis sets ranging from 6-311G(d) to cc-pVTZ. Ab initio calculations were performed using the CCSD(T)(fc) method with cc-pVDZ and cc-pVTZ basis sets. The equilibrium molecular geometries of **1** were fully optimized using "opt = very tight", and harmonic frequencies were then calculated at the minima to verify the nature of the stationary points. A comparative assessment of the CCN bending potential and barrier to linearity was obtained using HF, MP2(fc), B3LYP, and CCSD(T)(fc) with a common basis set, cc-pVTZ. For characterization of the normal modes of **1** and **2**, the total energy distribution (TED), which provides a measure of the internal coordinate contributions, was determined.[32]

Calculations for the isomerization/dimerization processes were conducted using B3LYP with a 6-311+G(2d) basis set. For open-shell singlet structures, calculations were performed at the UB3LYP level. Stability checks of wave functions were done for all calculated structures (minima and transition states (TSs)). For a better estimate of the relative energies of **1** and its isomers, single point CCSD(T)(full)/6-311+G(2d) calculations were performed for the B3LYP optimized structures, and relative Gibbs free energies (ΔG) were calculated by correcting the CCSD(T) total energies with corrections calculated at the B3LYP level. All calculations were performed on UP2000-ALPHA computers using Gaussian 98.[33]

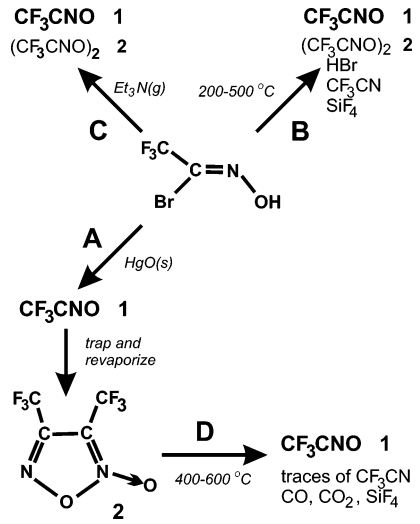

Figure 1. The four methods used to generate CF_3CNO (**1**) from the $CF_3BrC{=}NOH$ precursor. Method A (see text) is experimentally the simplest and leads to the purest **1**.

Results and Discussion

Generation, Identification, and Stability of CF_3CNO (1) and $(CF_3CNO)_2$ (2). Dehydrohalogenation methods to form dibromofuroxan, for example, reaction of $Br_2C{=}NOH$ in ether with HgO(s) or NH_3(g),[34] suggested the intermediacy of BrCNO and enabled us to demonstrate previously[15] the formation of BrCNO in the gas phase, albeit with concomitant formation of the furoxan dimer. This approach (Figure 1, method A), employing a gas−solid reaction, was adopted here, with $CF_3BrC{=}NOH$(g) passed at low pressure over HgO(s) placed, loosely, in a 10 cm long Pyrex tube. The reaction was rapid at room temperature, with $HgBr_2$(s) and H_2O(g) formed as byproducts, the latter being removed by employing a small amount of Drierite just after the reaction tube, and other volatile reaction products, for example, unreacted $CF_3BrC{=}NOH$, the ring dimer (**2**), and diethyl ether, appeared together with **1**. In a refinement of the experiment to remove the side products, a U-trap following the reaction tube was cooled to −126 °C (methylcyclohexane/liquid nitrogen slush). At this temperature, only **1** was observed in the gas phase, so clean IR spectra could be obtained, whereas, in the other methods (B → D) described below, other side products were identified.

Three other routes (Figure 1) were also employed, primarily to confirm the identity of **1** but also to establish that diethyl ether was not interfering. Method B, involving the direct pyrolysis of $CF_3BrC{=}NOH$ with HBr elimination, was conducted in a quartz tube loosely packed with quartz chips heated along 10 cm. The decomposition of $CF_3BrC{=}NOH$ began at 200 °C, yielding small amounts of **1** (identified by the distinctive strong peak at ∼2260 cm^{-1}) and HBr. At 400 °C, no starting material remained, with **1** as the major product, together with traces of HBr, CF_3CN (identified by its known IR spectrum[35]), a small amount of the furoxan (**2**), and ether. Further increases in temperature up to 500 °C resulted in increased CF_3CN, with SiF_4[36] also appearing, presumably resulting from the reaction of a CF_3 containing molecule with the quartz.

TABLE 1: Calculated Equilibrium Structures, Transition States and Barriers to Linearity, Total Energies, Dipole Moments, and Rotational Constants of CF_3CNO Using DFT (B3LYP)[a]

	B3LYP/ 6-311G(d)		B3LYP/ 6-311+G(d)		B3LYP/ 6-311G(2d)		B3LYP/ 6-311+G(2d)		B3LYP/ cc-pVDZ		B3LYP/ cc-pVTZ	B3LYP/ aug cc-pVTZ
parameter	min C_s	TS C_{3v}	min C_s	TS C_{3v}	min C_s	TS C_{3v}	min C_s	TS C_{3v}	min C_s	TS C_{3v}	min C_{3v}	min C_{3v}
C−C	1.462	1.460	1.4599	1.458	1.463	1.463	1.461	1.461	1.471	1.466	1.462	1.461
C−N	1.163	1.161	1.160	1.160	1.159	1.159	1.157	1.157	1.174	1.169	1.158	1.157
N−O	1.190	1.191	1.192	1.192	1.193	1.193	1.195	1.195	1.192	1.194	1.190	1.191
C−F(1)	1.342	1.343	1.345	1.346	1.340	1.341	1.343	1.343	1.342	1.345	1.341	1.343
C−F(2)	1.344	1.343	1.346	1.346	1.341	1.341	1.343	1.343	1.346	1.345	1.341	1.343
CCN	168.3	180.0	173.59	180.0	175.5	180.0	179.0	180.0	158.5	180.0	180.0	180.0
CNO	177.7	180.0	178.8	180.0	179.1	180.0	179.8	180.0	175.5	180.0	180.0	180.0
F(1)CC	111.1	111.0	111.2	111.2	111.0	111.0	111.1	111.1	111.0	111.0	111.0	111.1
F(2)CC	111.0	111.0	111.1	111.2	111.0	111.0	111.1	111.1	111.0	111.0	111.0	111.1
F(2)CCN dihedral	60.0	60.0	60.0	60.0	60.0	60.0	60.0	60.0	60.0	60.0	0	0
barrier to linearity (cm^{-1})	2.0		3.2		4.2		2.9		40.2		0	0
total energy of minimum (au)	−505.748 679		−505.764 033		−505.762 283		−505.777 083		−505.635 548		−505.804 294	−505.813 425
dipole moment (D)	0.63		0.62		0.74		0.78		0.53		0.76	0.78
rotational constants (GHz)	5.641 10		5.629 71		5.658 34		5.648 09		5.633 67		5.656 42	5.648 94
	1.481 82		1.475 16		1.475 55		1.473 62		1.490 93		1.475 63	1.475 11
	1.481 46		1.475 03		1.475 49		1.473 56		1.490 14		1.475 63	1.475 11

[a] Bond lengths in angstroms and bond/dihedral angles in degrees.

Method C (Figure 1), making use of the observation that nitrile oxides can be generated in solution from a suitable oxime or halogenated oxime with base,[1−5] involved the gas-phase reaction of the brominated oxime with triethylamine. A facile reaction occurred between gaseous $CF_3BrC{=}NOH$(g) and Et_3N-(g) with **1** and **2** being the resulting products in the gas phase.

The trapping of all products from method A at −196 °C (liquid nitrogen), followed by slow warming, was undertaken to investigate both the ability of **1** to revaporize as the monomer and its possible dimerization from which an IR spectrum of pure **2** could be obtained. Upon warming, **1** gradually appeared at about −130 °C, followed by other volatile products, mainly diethyl ether appearing above −100 °C, followed by the appearance of **2** at about −90 °C, with, finally, pure **2** being observed at 0 °C and above. Given the earlier work on the dimerization of simple nitrile oxides,[1−5,15,19] this result was not unexpected and confirms the solution observation[12] that, in the absence of trapping dipolarophiles, **1** dimerizes. A further refinement used a trap at −126 °C followed by a second trap at −196 °C; the first trap captured most of the ether and H_2O, and the second trap retained almost pure **1**. The traps were isolated (valve), and the −196 °C trap was slowly warmed in stages to room temperature to permit dimerization to occur. An IR spectrum of this material revealed the presence of some diethyl ether which was removed by cooling the trap to −77 °C (dry ice) and pumping off the ether, leaving pure furoxan (**2**) for both IR (gas) and Raman (liquid) investigation.

As noted earlier, certain furoxans, notably the dicyano-[17] and dimethylfuroxans,[22] undergo relatively clean thermolytic cycloreversion to give back the corresponding nitrile oxide. This reaction (Figure 1, method D), involving the thermolysis of **2** (collected as described above), was carried out in a quartz tube heated over 10 cm, which was sparsely filled with quartz chips. At about 400 °C, **1** started to appear. Increasing the temperature to 500 °C gave mainly **1** with some residual **2**, and at 600 °C, the spectrum consisted of almost pure **1** with traces of CF_3CN, CO, and CO_2. Under some circumstances, for example, slower flow rates, higher temperatures (e.g., 700 °C), and the use of more quartz chips in the pyrolysis tube, increased amounts of CF_3CN were seen together with traces of SiF_4.

A comment is merited here about the fact that the brominated oxime precursor is an etherate complex. Vaporization studies conducted using different temperature traps suggest that, at the pressures at which we are working (300−1000 mTorr), the oxime and ether exist as independent molecules in the gas phase. In the three methods (A → C) involving chemical or thermal elimination of HBr from $CF_3BrC{=}NOH$, free ether was recognized in the IR spectrum or was removed in a cold trap. Method D, direct formation of **1** from the pure dimer (**2**), served to confirm identification of ether-free **1** in the spectra.

Computational Investigation of the Structure of 1. The structures of simple nitrile oxides are a continuing challenge for ab initio methods, issues focusing on the role played by different electron correlation and basis set size effects.[15,17,19−22,37−39] Very high levels of theory were required to reproduce the potential functions and spectroscopically observed quasi-linear behavior of ClCNO[16,37] and BrCNO[16,38] and the linear/quasi-linear nature of NCCNO.[18,39] Table 1 shows the calculated structures of **1** (both minima and, where necessary, the linear TS) using DFT (B3LYP) with basis sets ranging from 6 -311G(d) to cc-pVTZ. Table 2 shows the ab initio (CCSD-(T)) results with basis sets from cc-pVDZ to cc-pVTZ. The principal difference between the DFT and ab initio results is that B3LYP (except with the cc-pVDZ basis set) gives a linear or close-to-linear CCNO frame, whereas CCSD(T) favors a bent structure. Although this difference between methods (DFT and ab initio) appears large, it has to be taken in the context of a very flat bending potential (below) and the difficulty in correctly describing the electron correlation for such an electron rich system with large amplitude motion.

The B3LYP calculations, with various Pople triple split valence basis sets, show only incremental changes in structural parameters; for example, increasing the basis set size brings the CCN angle closer to linear, with the introduction of diffuse functions very slightly shortening the CC and CN bonds and increasing the NO bond. Similar basis set effects using other exchange correlation functionals have been observed for the quasi-symmetric top disiloxane.[40] Overall, with the Pople basis sets used here, the CCN angle is in the range 168−179°, with a barrier to linearity of <4.2 cm^{-1} (Table 1). There is a discontinuity with the cc-pVDZ basis set, which shows a more bent structure, longer bond lengths, and the barrier increased to 40.2 cm^{-1}. The B3LYP/cc-pVTZ result more closely mimics

TABLE 2: Calculated Equilibrium Structures, Transition States and Barriers to Linearity, Total Energies, Dipole Moments, and Rotational Constants of CF_3CNO Using CCSD(T)[a]

	CCSD(T)(fc)/ cc-pVDZ		CCSD(T)(fc)/ cc-pVTZ	
parameter	min C_s	TS C_{3v}	min C_s	TS C_{3v}
C−C	1.492	1.481	1.479	1.472
C−N	1.200	1.182	1.179	1.167
N−O	1.196	1.202	1.193	1.197
C−F(1)	1.338	1.340	1.330	1.332
C−F(2)	1.341	1.340	1.334	1.332
CCN	142.4	180.0	148.9	180.0
CNO	171.7	180.0	173.3	180.0
F(1)CC	110.4	110.7	110.6	110.7
F(2)CC	110.9	110.7	110.8	110.7
F(2)CCN dihedral	60.1	60.0	60.0	60.0
barrier to linearity (cm^{-1})	485.8		174.2	
total energy of minimum (au)	−504.474 210		−504.971 452	
dipole moment (D)	1.11		1.43	
rotational constants (GHz)	5.657 70		5.721 06	
	1.533 60		1.527 56	
	1.532 40		1.526 37	

[a] Bond lengths in angstroms and bond/dihedral angles in degrees.

the Pople basis set values; for example, compare 6-311+G(2d) with aug-cc-pVTZ, with the structure now predicted to be linear.

The CCSD(T)(fc) calculations predict the molecule to be bent, albeit with the barrier to linearity decreasing from 486 to 174 cm^{-1} upon moving from a double-ζ (DZ) to a triple-ζ (TZ) basis set. Recent CCSD(T) calculations on other XCNO species (X = F,[21] Cl,[37] Br,[38] and NC[39]) have demonstrated that a DZ basis set is inadequate, whereas a TZ basis set, giving distinct decreases in bond lengths (and barrier) compared to DZ, more closely approaches the complete basis set (CBS) limit. This trend in decreased bond lengths is also noted here (Table 2). Such TZ (and larger) calculations successfully predict XCN bending potentials and bending energy levels for several small nitrile oxides.[16,18,37−39] This DZ to TZ effect concurs with concerns[41] about the use of CCSD(T)/cc-pVDZ to provide the "correct" geometries.

The clear conclusion from both the B3LYP and CCSD(T)-(fc) calculations is that **1** has a very flat potential in the bending mode, with a small barrier to linearity. Figure 2 shows the CCN bending potential at the CCSD(T)(fc)/cc-pVTZ level together with, for comparison, HF, MP2, and B3LYP calculations with the same basis set. These were obtained by fixing the CCN angle at 10° intervals and optimizing the structures. The fitted potential for CCSD(T)(fc)/cc-pVTZ has the following form (where ρ is the deviation in degrees from linearity):

$$V(\mathrm{cm}^{-1}) = 174.1 - 0.357\rho^2 + 0.000\,183\,7\rho^4$$

The comparable potential for the H-substituted analogue, CH_3CNO, with the same basis set is given by

$$V(\mathrm{cm}^{-1}) = 0.210\rho^2 + 0.000\,180\,1\rho^4$$

The CCSD(T)(fc)/cc-pVTZ potential for **1** is thus somewhat different from that of CH_3CNO which has a linear CCN group both theoretically and experimentally[42] and substantially different from that for the bent FCNO molecule.[20,21] However, it is comparable to the bending potentials for the strongly quasi-linear ClCNO and BrCNO molecules,[16,37,38] suggesting that **1** is a strongly quasi-symmetric top. The other curves (Figure 2) are provided to illustrate the effects of method and electron

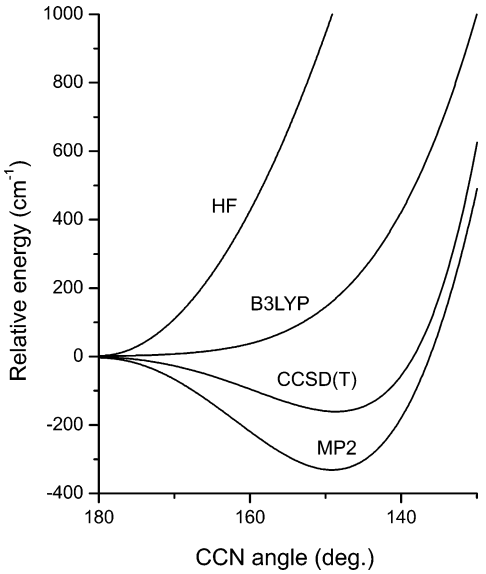

Figure 2. Calculated (HF, MP2(fc), B3LYP, and CCSD(T)(fc)) CCN bending potential for CF_3CNO (**1**) with a common basis set, cc-pVTZ.

correlation on the shape of the potential, with HF clearly giving a much narrower potential, favoring a truly linear structure, while B3LYP more readily demonstrates large amplitude motion. Curiously, but as noted before,[21,37−39] the MP2 curve is similar to that using CCSD(T), perhaps reflecting a "mutual cancellation of the higher-order correlation corrections to the total energy". The MP2 barrier to linearity is 339 cm^{-1} with a CCN angle of 149°. The, albeit not large, differences between B3LYP and CCSD(T)(fc) for **1** may reflect subtle differences in the handling of electron correlation by DFT, a topic recently reviewed[43,44] in which B3LYP is noted to mimic pair−pair-coupling effects and covers a large proportion of three-electron correlation effects.

Clearly, the nature of the substituent, X, plays a strong role in determining the structure of molecules of the type XCNO. A natural population analysis for FCNO[20] and other substituted nitrile oxides suggested that a π donor and a σ acceptor (e.g., F) favors a bent XCNO group. A similar analysis for **1** at the B3LYP/6-311G(2d) level confirms that the CF_3 group is also electron withdrawing (i.e., a $-I_\sigma$ effect) but has negative hyperconjugation which donates electron density from the filled π orbitals into the C−C bond, contributing more to a linear structure.

Infrared Spectroscopy of 1. Method A (Figure 1), the reaction between $CF_3BrC{=}NOH$(g) and HgO(s) with a following trap at −126 °C, leads to the cleanest formation of **1**. The IR spectrum is shown in Figure 3, with experimental and theoretical (unscaled, harmonic) band positions, assignments, and TEDs given in Table 3. The theoretical values shown describe the limiting cases, linear (B3LYP/cc-pVTZ) and bent (CCSD(T)(fc)/cc-pVDZ) CCNO frames, with the TED values based on a linear CCNO structure.

The IR spectrum of the methyl analogue CH_3CNO with a known C_{3v} structure[42] shows a clear distinction between parallel ($A_1 \leftarrow A_1$) and perpendicular ($E \leftarrow A_1$) type bands,[22] but this is not evident for **1** where the bands show more complex structure. For the purposes of discussion, we consider **1** as a quasi-symmetric top with the 15 normal modes transforming as $5A_1 + 5E$, all being IR active. There are a limited number of observed bands; as indicated in Table 3, only three or four fundamentals are predicted to have significant intensity. Their complicated profiles, similar to those observed with other small

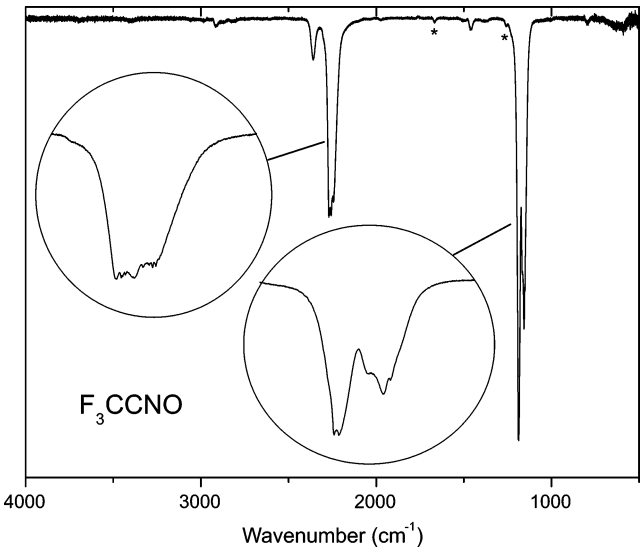

Figure 3. Gas-phase infrared spectrum of CF_3CNO (**1**) obtained from method A (with use of trapping, see text), showing expansions of the most prominent bands. The asterisks indicate the most intense peaks of the furoxan dimer (**2**).

XCNO molecules (X = Br,[15] Cl,[19] NC,[17] CH_3[22]) can arise from several sources. An additional issue, apparent from the TEDs in Table 3, is the significant coupling of energy making the assignment of fundamentals and comparisons with similar molecules, for example, CF_3CN, more difficult.

Such nitrile oxides typically have a prominent band around 2250 cm^{-1} arising from the CNO asymmetric stretch (ν_{as}(CNO)), although none clearly exhibit the *PQR* (*PR*) structure expected for a parallel transition in a symmetric top (linear molecule). This band in **1** is no exception, it being broad and multistructured (inset to Figure 3), although *R* and *Q* branches can be discerned at 2270 and 2266 cm^{-1}, respectively. The complex structure, hampering any identification of the *P* branch, could arise from hot bands of the lowest bending frequency, leading to multiple *Q*-branch structure shaded to lower frequency. A similar, but better resolved, structure has been observed in CF_3CN.[45] Alternatively, or in addition, this structure (especially that centered around 2243 cm^{-1}) could arise from a combination band ($\nu_2(1459) + \nu_4(795)$) which has borrowed intensity through a Fermi resonance with ν_{as}(CNO). From the TED, Table 3, it is clear that the fundamental, $\nu_1(a_1)$, has localization in the CN stretch. The corresponding ν_s(CNO) band is, compared to the same mode in other nitrile oxides, very much weaker and is shifted to 1459 cm^{-1}, similar to that in NCCNO but ~110 cm^{-1} higher than that in the Br- and Cl-nitrile oxides. This mode, $\nu_2(a_1)$, is best described as the NO stretch.

The two strong bands at 1188 and 1156 cm^{-1} are associated with the three CF stretches ($\nu_3(a_1)$ and ν_6(e)). The TED clearly shows coupling of these two modes with the CF_3 deformation and also, in the a_1 mode, to the ON and CC bond stretches. At issue here is the relative ordering; a parallel transition in a symmetric top is clearly distinguishable from a perpendicular transition in the ideal case, but hot bands and, in the case of the perpendicular transition, the magnitude (and sign) of the Coriolis coupling constant (ξ) can lead to irregular band structure which certainly obfuscates the assignment here. Again, such complications were seen in CF_3CN[45,46] with, in addition, overtones and combination bands affecting the band shapes. The CF_3 a_1 and e stretches in CF_3CN are located at 1227 and 1214 cm^{-1}, respectively.[45−47] In the case of **1**, we are inclined to switch this ordering based on the calculated intensities, placing ν_6(e) at 1188 cm^{-1} and $\nu_3(a_1)$ at 1156 cm^{-1}. Also, all the frequency calculations we have done, including the subset in Table 3, suggest this ordering, although the e mode is calculated, by B3LYP, to be low. A B3LYP/6-311+G(2d) calculation performed on CF_3CN also calculates the perpendicular band ~50 cm^{-1} too low.

Below 1000 cm^{-1}, three very weak bands can be assigned to **1**. That at 795 cm^{-1} is assigned to $\nu_4(a_1)$, a mode that is strongly mixed, mainly CF stretching and deformation, and CC stretching. The comparable CC stretch in CF_3CN is at 802 cm^{-1}, also mixed with CF stretches; that in CH_3CNO is at 785 cm^{-1}. Two broader weak bands at 634 and 584 cm^{-1} are, from inspection of many spectra, associated with **1**. The signal/noise in this region is poor, and there is no discernible structure. These bands could be assigned to the ν_7(e) (CF_3 asymmetric deformation/rock) and ν_8(e) (CNO bend) fundamentals, but the problem here is that the B3LYP calculations (Table 3) predict them to be ~50 cm^{-1} lower. An alternative explanation is that they are combination bands involving the lowest (and unobserved) bending mode, for example, $\nu_7 + \nu_{10}$ for the band at 634 cm^{-1} and $\nu_8 + \nu_{10}$ for the band at 584 cm^{-1}, assuming a ν_{10} frequency of ~50 cm^{-1}.

Apart from the putative combination band ($\nu_2 + \nu_4$, ~2243 cm^{-1}) mentioned before, other weak features have been observed which are consistently present and track the strong bands in the many IR spectra of **1** from different preparative methods. These are assigned to overtone or combination bands and are listed in Table 3, with tentative assignments. Chief among these is the distinct band at 2360 cm^{-1} which we assign to $2\nu_3$, which seems to have borrowed intensity from the adjacent $\nu_1(a_1)$ band.

A bent structure, predicted by the CCSD(T)(fc) and B3LYP/6-311+G(2d) calculations, would remove the degeneracies, although, for the latter, as with other B3LYP calculations (Table 1), the degeneracy breaking is negligible as the structure is so close to linear. The CCSD(T)(fc)/cc-pVDZ structure, as the most bent, predicts a splitting of 15 cm^{-1} for the (formerly) E modes. The narrow range of frequencies associated with the degeneracy breaking and the complicated observed band profiles makes it difficult, from the experimental IR spectrum, to definitively state whether the CCNO frame is linear or bent.

Computational Investigation of the Structure of 2. Structural studies of simple disubstituted furoxans are limited, although there are several recent ab initio calculations on such structures with emphasis placed on the need to correctly assess dynamical electron correlation effects.[48−51] The calculated framework structure of **2** at the B3LYP/6-311+G(2d) level is shown in Figure 4 and clearly shows the long endocyclic NO bond which is a point of scission upon thermolysis to give the monomer (**1**). This bond length, which is notoriously difficult to treat properly by computational methods (see, for example, Table 2 in ref 49), is in the appropriate range, suggesting that B3LYP with the present basis set is an appropriate level of theory for this system. The ring is planar. We will not belabor a discussion of the structure at this point, since we are preparing a more detailed discussion on all the disubstituted furoxans (H, Cl, Br, NC, CH_3, and CF_3) which we have investigated, with particular emphasis on calculated/experimental structures, vibrational spectroscopy (IR and Raman), and charge distributions.[52]

Infrared Spectroscopy of 2. The IR spectrum of **2** is shown in Figure 5, with experimental and theoretical frequencies, and the TED given in Table 4. As noted for various alkyl- and arylfuroxans,[53−55] fundamentals associated with the furoxan ring

TABLE 3: Experimental[a] and Calculated[b] Vibrational Frequencies (cm^{-1}) of CF_3CNO

	CCSD(T)/cc-pVDZ		B3LYP/cc-pVTZ		B3LYP/6-311+G(2d)			
exptl (gas)	freq(sym)	intens[c]	freq(sym)	intens[c]	freq(sym)	intens[c]	assignt	TED%[d]
3400							$\nu_1 + \nu_3$	
2913							$2\nu_2$	
2360							$2\nu_3$	
2266(s)	2281(A′)	634.9	2457(A_1)	827.1	2439(A′)	873.2	ν_1(A_1)	79, CN st; 15, ON st; 6, CC st
2243							$\nu_2 + \nu_4$	
1976							$\nu_4 + \nu_6$	
1459(vw)	1497(A′)	44.4	1503(A_1)	0.2	1490(A′)	0.3	ν_2(A_1)	64, ON st; 27, CC st; 5, CN st
1188(s)	1255(A′)	360.5	1155(E)	312.4	1131(A′)	329.2	ν_6(E)	83, CF_3 as st; 11, CF_3 as def; 5, CF_3 rock
	1240(A″)	332.2			1131(A″)	327.8		
1156(s)	1178(A′)	483.2	1139(A_1)	679.5	1127(A′)	714.8	ν_3(A_1)	42, CF_3 st; 30, CF_3 def; 14, ON st; 9, CC st
795(vw)	800(A′)	4.4	777(A_1)	19.0	769(A′)	16.7	ν_4(A_1)	56, CF_3 st; 23, CF_3 def; 14, CC st; 4, CN st
634(vw)	621(A′)	46.9	584(E)	5.8	579(A′)	5.3	ν_7(E) or $\nu_7 + \nu_{10}$ (see text)	39, CF_3 as def; 34, CF_3 rock; 14, CF_3 st; 13, CNO bend
	582(A″)	7.7			579(A″)	5.3		
584(vw)	555(A′)	1.4	534(E)	3.7	531(A′)	2.7	ν_8(E) or $\nu_8 + \nu_{10}$ (see text)	87, CNO bend; 13, CF_3 as def
	507(A″)	6.2			531(A″)	2.7		
	469(A′)	3.4	454(A_1)	1.0	451(A′)	1.3	ν_5(A_1)	44, CF_3 def; 44, CC st; 8, CN st; 4, ON st
	398(A″)	0.0	402(E)	0.1	398(A′)	0.2	ν_9(E)	59, CF_3 rock; 35, CF_3 as def; 4, CNO bend
	390 (A′)	3.1			397(A″)	0.2		
	105(A′)	2.3	20(E)	0.8	30(A′)	1.1	ν_{10}(E)	100, CCN bend
	39(A′)	0.2			27(A″)	1.1		

[a] Band positions taken from the maxima or sharp features of the bands. [b] Unscaled harmonic frequencies. [c] In kilometers per mole. [d] Characterization of the fundamentals; TED (total energy distribution). Abbreviations: stretch (st); asymmetric (as); deformation (def).

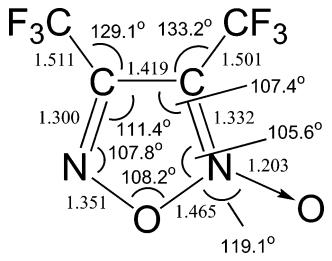

Figure 4. Calculated (B3LYP/6-311+G(2d)) structure of the furoxan dimer ($(CF_3CNO)_2$, **2**).

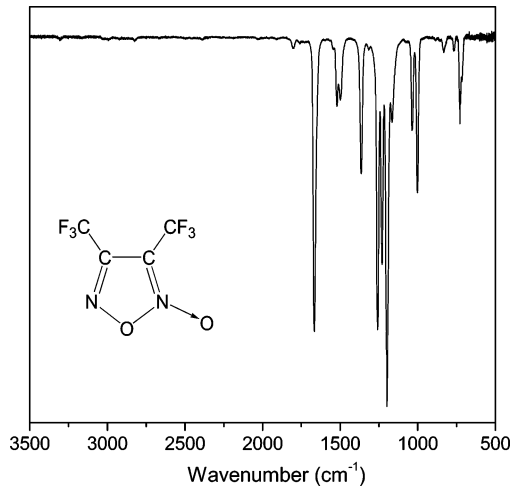

Figure 5. Gas-phase infrared spectrum of the furoxan dimer ($(CF_3CNO)_2$, **2**).

do not occur above 1750 cm^{-1}. The same holds for the dichloro-,[19,51,56] dibromo-,[15,50] and dicyanofuroxans.[57] An assignment of the IR bands is assisted by recourse to known furoxan data and the B3LYP/6-311+G(2d) calculations. All previous work shows a strong absorption band in the 1700−1600 cm^{-1} region characteristic of the furoxan group and assigned to the C═N → O vibration. This band occurs in **2** at 1667 cm^{-1} (1662 cm^{-1} in dimethylfuroxan[52]). Most aryl-, acyl-, and alkyl-substituted furoxans also show a second C═N based stretch, generally weaker, between 1500 and 1600 cm^{-1}, although this was not observed in the case of dibromo-,[15] dichloro-,[19] and dimethylfuroxan.[52] In **2**, this mode is observed as a weak band at 1521 cm^{-1}. Although the normal modes are strongly mixed (see the TED), both show C═N character, with the higher possessing considerable N → O character. For both dibromo-[15] and dichlorofuroxan,[19] modes having C—X (X = Br, Cl) character were not observed above 540 cm^{-1}, with all higher fundamentals assigned to ring stretching and ring deformation motions. In the case of **2**, the CF_3 substituent leads to strong CF stretches in the 1160−1260 cm^{-1} region, with the CF_3 deformations occurring below 750 cm^{-1}. In Table 4, the assignments given divide between the CF_3 substituent and the ring (albeit with considerable mixing). We make no attempt at this stage to provide comparisons to other disubstituted furoxans. As noted above, a complete vibrational (IR/Raman) study of this molecule together with those of other disubstituted furoxans will be published separately.

Isomerization of the CF_3(NCO) Isomers. Monomolecular (e.g., isomerization) and intermolecular (e.g., dimerization) processes are possible loss processes for nitrile oxide (**1**), relevant to the relationship of **1** to other pseudohalide isomers, for example, isocyanate (the sole species for which some experimental data are available[58,59]), cyanate, fulminate, and other species for which no experimental work is available. DFT calculations were performed to provide information on the thermodynamic and kinetic stability of these isomers. Minima and TSs on the singlet surface were calculated at the B3LYP/6-311+G(2d) level, a method which gives good agreement for the known structure of CF_3NCO[58,59] (Table 5). Improved estimates of the total and relative energies were obtained from CCSD(T)(full)/6-311+G(2d) single point energy calculations at the B3LYP geometries. Zero point vibrational energies (ZPEs) were included. Since, for the relative energies, the B3LYP and CCSD(T) calculations give qualitatively the same result, the discussion will focus on the CCSD(T) values.

Six isomers including four pseudohalide derivatives are identified as minima on the B3LYP singlet surface. These isomers and the relative free energies (ΔG) are shown in Figure

TABLE 4: Experimental and Calculated Vibrational Frequencies (cm^{-1}) of the Furoxan ($(CF_3CNO)_2$, 2)

	calculated		
exptl IR[a]	freq[b]	intens[c]	TED%[d]
1667(vs)	1692	499.8	62, NO* st; 29 CN st
1521(m)	1553	42.7	74, CN st; 11 CC st
1499(m)	1509	74.5	49, CC rst; 30, CC st
1365(m)	1373	106.1	31, CC st; 26, CN st, 19, r b
1259(vs)	1252	324.6	27, CF_3 st; 15, CF_3 s def; 14, CC st; 12, CN st; 11, CC rst
1230(s)	1207	273.1	59, CF_3 st; 11, CN st
1202(m,sh)	1167	64.7	57, CF_3 st; 11, CN st
1199(vs)	1153	552.3	81, CF_3 st; 11, CF_3 as def
1166(m)	1151	91.8	65, CF_3 st; 10, CF_3 as def
n.o.[e]	1138	0.0	81, CF_3 st; 11, CF_3 as def
1036(m)	1058	104.9	54, ON st; 15, CF_3 st; 13, r b
1003(m)	1012	178.2	37, r b; 33, CF_3 st
833(vw)	843	24.0	45, r b; 20, ON, st; 13, CF_3 st
n.o.	764	2.7	40, CF_3 st; 20, CF_3 s def; 11, r b
n.o.	753	2.1	38, r t; 22, CC w; 18, CF_3 rock; 17, NO* w
767(vw)	728	14.8	27, CF_3 st; 21, CF_3 s def; 14, NO* b; 10, CC b
729(m)	719	42.5	39, CF_3 s def; 26, CF_3 st; 10, ON st
n.o.	652	0.2	38, NO* w; 19, CF_3 rock; 18, r t; 13, CC w
n.o.	578	0.0	36, CF_3 as def; 19, CF_3 rock; 15, r t; 14, NO* w; 14, CF_3 st
n.o.	570	1.3	39, CF_3 as def; 15, CF_3 st; 12, CF_3 rock; 11, ON st
n.o.	548	3.0	62, CF_3 as def; 14, CF_3 st; 10, ON st
n.o.	543	0.4	59, CF_3 as def; 25, r t; 13, CF_3 st
463(vw)	479	15.8	50, ON st; 27, CF_3 as def; 12, NO* b
n.o.	439	1.1	44, CF_3 as def; 24, CF_3 rock; 20, r t; 11, CC w
428(vw)	433	5.7	26, CF_3 as def; 18, CC st; 15, CF_3 s def; 12, CF_3 rock; 11, ON st
n.o.	413	2.2	32, CF_3 rock; 28, CF_3 as def; 16, NO* w; 14, r t; 10, CC w
n.o.	372	0.0	23, CF_3 rock; 19, CC st; 15, NO* b; 13, CF_3 s def; 10, CF_3 as def
n.o.	307	0.8	51, CF_3 rock; 15, CC st; 10, CC r st; 10, CF_3 as def
n.o.	286	0.0	30, CC st; 20, r b; 17, CF_3 s def; 15, CF_3 rock
n.o.	250	0.1	50, r t; 38, CF_3 rock; 10, NO* w
n.o.	184	2.6	54, CC b; 37, CF_3 rock
n.o.	145	3.9	77, CC w; 25, CF_3 rock
n.o.	118	0.1	80, CC b; 11, CF_3 rock
n.o.	98	0.1	50, CC w; 19, r t; 19, CC t
n.o.	57	0.1	83, CC t; 14, CC w
n.o.	15	0.0	98, CC t

[a] Gas phase; additional very weak features at 716, 1318, and 1547 cm^{-1} associated with **2**. [b] Unscaled harmonic frequencies, calculated at the B3LYP/6-311+G(2d) level. [c] IR intensities in kilometers per mole. [d] Characterization of the fundamentals; TED (total energy distribution). Only contributions above 10% are given. Abbreviations: stretching (st), ring stretching (rst), ring (r), torsion (t), bending (b), symmetric deformation (s def), asymmetric deformation (as def), and wag (w). NO* is the exocyclic N → O. [e] n.o. (not observed).

TABLE 5: Calculated Total and Relative Energies of the $CF_3(NCO)$ Isomers and Transition States

			relative energy[a] B3LYP/6-311+G(2d) (kcal/mol)		relative energy[a] CCSD(T)//B3LYP/6-311+G(2d) (kcal/mol)	
struct no.	minimum or TS	total energy (au) B3LYP/6-311+G(2d)	ΔE	ΔG	ΔE	ΔG
			Minima			
3	CF_3-NCO	−505.888 546	0.0	0.0	0.0	0.0
4	CF_3-OCN	−505.836 008	32.6	33.1	27.1	27.6
1	CF_3-CNO	−505.777 083	69.2	68.3	71.2	70.2
5	CF_3-ONC	−505.745 359	88.5	88.9	83.1	83.6
6	$CF_3-C(O)N$	−505.741 734	90.6	90.8	83.9	84.2
7	$CF_3-N(OC)$	−505.706 531	112.0	112.6	106.0	106.6
			Transition States			
8	**4** ↔ **6**	−505.719 131	104.3	104.3	105.4	105.4
9	**3** ↔ **6**	−505.715 950	105.2	105.3	105.9	106.0
10	**5** ↔ **4**	−505.697 374	117.0	117.6	111.5	112.1
11	**7** ↔ **3**	−505.689 970	121.1	121.6	116.3	116.8
12	**6** ↔ **1**	−505.666 283	136.1	136.5	137.2	137.6
13	**7** ↔ **1**	−505.652 708	145.1	145.6	144.3	144.8
14	**5** ↔ **1**	−505.611 644	170.7	171.1	170.1	170.6

[a] Energy (ΔE) corrected with ZPE and Gibbs Free energy (ΔG) at 298.15 K and 1 atm, relative to that of the thermodynamically most stable isomer CF_3NCO (**3**); all electrons are included in the electron correlation calculations, that is, CCSD(T)(full); ZPE and thermal corrections are calculated at the B3LYP/6-311+G(2d) level.

6, together with the connecting TSs. The structures of all minima and TSs are shown in Figure 7; for clarity, the CF_3 group is shown as a single entity. As often noted, the pseudohalide group is nonlinear. Isocyanate (CF_3NCO, **3**) is the most stable structure, followed in order of thermodynamic stability by the cyanate (CF_3OCN, **4**), nitrile oxide (CF_3CNO, **1**), fulminate (CF_3ONC, **5**), oxazirine ($CF_3C(ON)$, **6**), and oxaziridinilidene ($CF_3N(OC)$, **7**) isomers. The minima for **3**, **4**, and **1** lie in deep

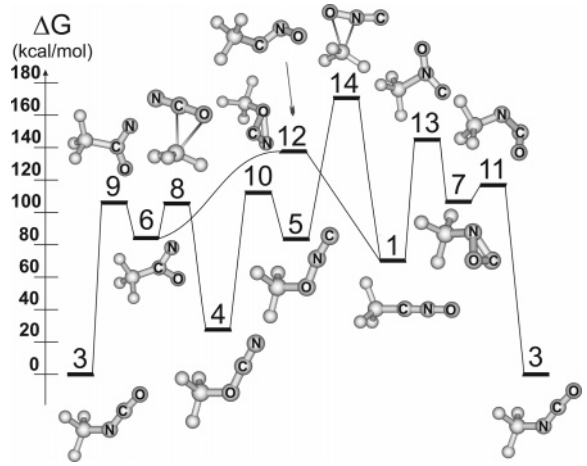

Figure 6. Calculated (B3LYP/6-311+G(2d)) isomerization pathways of the $CF_3(NCO)$ isomers.

wells with the lowest barriers to isomerization of 106.0 (TS **9**), 77.8 (TS **8**), and 67.4 (TS **12**) kcal/mol, respectively. This kinetic stability concurs with the present IR observation of **1** and the spectroscopic measurements (IR/microwave) on **3**.[58,59] Cyanate (**4**) has not been observed experimentally but is predicted to be stable and a viable target for experiment. The calculations suggest that, at higher temperatures, **4** can isomerize into **3** via TSs **8** and **9**, and **1** can isomerize into **3** by two routes, either via TSs **12** and **9**, or via TSs **13** and **11**, although the intermediate **7** on the latter route is not predicted to be stable (below). We note that the isomerization of **4** and the TS (**12**, **9**) route for the isomerization of **1** both proceed through the common intermediate **6**. CCSD(T)(full)/6-311+G(2d)//B3LYP/6-311+G(2d) calculations (not shown) of dissociation energies for species **3**, **4**, and **1** suggest that, for spin-allowed processes, the lowest dissociation routes are some 20−30 kcal/mol lower in energy than the isomerization processes. For **1**, the room-temperature dissociation energy to $^1CF_3CN$ and ^1O is 45.7 kcal/mol compared to the isomerization barrier (to **3**) of 67.4 kcal/mol at the same level. Although traces of CF_3CN were observed in the thermolysis routes (methods B and D), it is feasible that it results from decomposition of the furoxan. Bimolecular loss routes to the furoxan are, as noted in the next section, much more favored.

The higher energy species, oxazirine (**6**) and the two other minima **5** and **7**, are in much shallower wells. Fulminate (**5**) isomerizes with a barrier (TS **10**) of 28.5 kcal/mol into the thermodynamically more stable **4**. Both the calculated barriers and lowest bond dissociation energy (which is higher, 37.7 kcal/mol) suggest that **5** could be generated at lower temperatures. The intermediate **6** which also has a high dissociation pathway (84.1 kcal/mol) can isomerize into the stable species **3** and **4** with barriers of 21.8 (TS **9**) and 21.2 (TS **8**) kcal/mol, respectively. This suggests that this structure is not stable at ambient temperature, although, interestingly, it has been postulated as an intermediate in the reaction between CF_3CN and O^1D.[60] The highest lying minimum **7** has a very low barrier (TS **11**) to isomerization (10.2 kcal/mol) to **3**, and the long N−C and N−O distances in **7** (Figure 7) suggest a facile dissociation. This process, yielding $^1CF_3N$ and ^1CO, is exothermic (−31.2 kcal/mol), suggesting that **7** is neither thermodynamically or kinetically stable.

The geometries for the TSs, illustrated in Figure 6, details in Figure 7, are much in keeping with those structures involved in the isomerization processes for the $CH_3(NCO)$ isomers,[22] the rearrangements occurring via either T-shaped structures or three-membered rings.

Dimerization of CF_3CNO (1) to the Ring Furoxan (2). The most facile loss processes for small nitrile oxides in the absence of a dipolarophile is dimerization to stable five-membered ring structures (furoxans),[1−5,15,19,20,22] a special type of [3 + 2] dipolar cycloaddition. The mechanism has long been the subject of discussion (see ref 61 for reviews), with the main issues relating to a concerted one-step process[62] or a sequential two-step process.[63] Our recent experimental and theoretical work on the dimerization of ClCNO[19] and CH_3CNO[22] suggested a two-step process with a Firestone-like intermediate. More recent theoretical work suggests the involvement of a 1,2-dinitrosoalkene intermediate,[48] and experimental evidence for a dinitrosobut-2-ene species has been demonstrated in the photolysis of dimethylfuroxan in an Ar matrix.[64] An important theoretical contribution has identified, on the nitrile oxide to furoxan dimerization surface, dinitrosoalkene intermediates with considerable diradical character.[65]

From our experimental work (vide supra), the dimerization of pure **1** occurs readily at close to room temperature, producing **2** exclusively, in accord with previous observations in solution.[12] Although a 1,4-dioxa-2,5-diazine species was also observed in the solution work, only a limited number of theoretical studies have considered other nitrile oxide dimerization products,[65,66] We thus investigated, using B3LYP and UB3LYP, three possible dimerization processes for **1**, namely, the relatively facile and experimentally observed reaction leading to the furoxan (**2**) and two other processes, one leading to the isomeric structure of furoxan (1,2,4-oxadiazole-4-oxide, **15**) and the other to 1,4-dioxa-2,5-diazine (**16**). The free energy pathways for these processes are shown in Figures 8 and 9, with the calculated structures of minima and TSs shown in Figure 10 and the calculated energies/relative energies of all species given in Table 6.

The dimerization pathway to the furoxan (**2**) (Figure 8) via the initial rate-determining TS **21** is a stepwise mechanism proceeding, in sequence, through the 1,2-bis(trifluoro)dinitrosoalkene-like intermediates **18** and **17** and TSs **19** and **20**, all having diradical character, that is, open-shell singlets, to the stable, closed-shell furoxan. Initial $\langle S^2 \rangle$ values (Table 6) for the diradical stationary points range from 0.936 to 1.020 and become 0.131 to 0.187 after spin annihilation, although TS **21**, the first contact of the two monomers, has an $\langle S^2 \rangle$ value of 0.131 (0.003 after annihilation). As the two closed-shell monomers come together, the first step proceeds through TS **21** (ΔG barrier, 25.0 kcal/mol) with an extended nonplanar structure (C−C distance, 1.963 Å; NCCN dihedral angle, 118°). This TS rotates to form a pure diradical species, the *cis*−*trans*−*cis* (*ctc*)-dinitrosoalkene nonplanar intermediate (**18**) (endothermic by 4.3 kcal/mol with respect to the two separated nitrile oxides), where the C−C bond length has closed to 1.490 Å and the NCCN dihedral has reduced to 105.7°. **18** leads with a small barrier (1 kcal/mol) via the singlet diradical TS **19** to the *cis*−*cis*−*cis* (*ccc*)-dinitrosoalkene (**17**) with the NCCN dihedral gradually decreasing from **18** (106°) through **19** (80°) to **17** (43°). With a relatively low energy (9.6 kcal/mol) rotation around the C−C bond, TS **20** (only 29.3° off planar) can then close to the planar furoxan (**2**). The rate-determining step in the monomer cyclodimerization is the first at TS **21** with a free energy barrier of 25.0 kcal/mol, suggesting, as observed, dimerization at room and higher temperatures. The overall pathway is similar to the diradical route previously determined for CH_3CNO.[65] We would add that other stationary points, including planar 1,2-dinitrosoalkene structures, have also

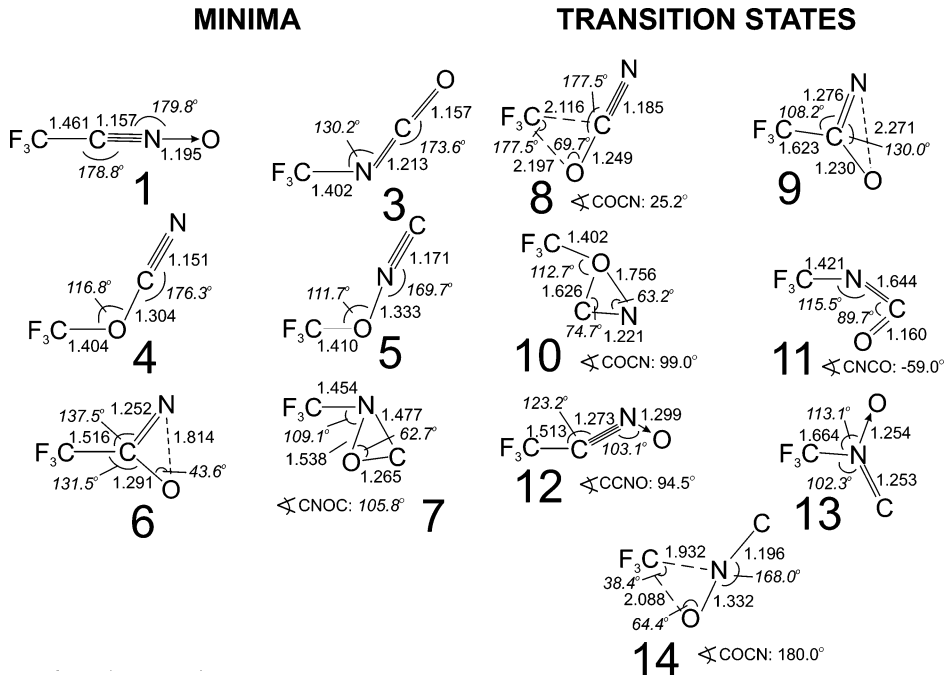

Figure 7. Calculated (B3LYP/6-311+G(2d)) structures of the minima and TSs for the $CF_3(NCO)$ isomers.

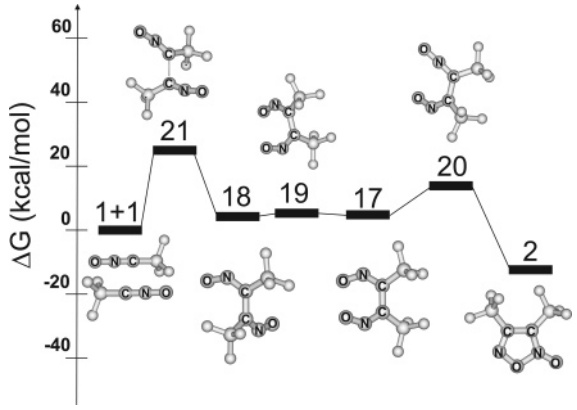

Figure 8. Calculated (UB3LYP/6-311+G(2d)) relative free energies (kilocalories per mole) of the minima and TSs in the dimerization pathway leading from **1** to the furoxan product (**2**).

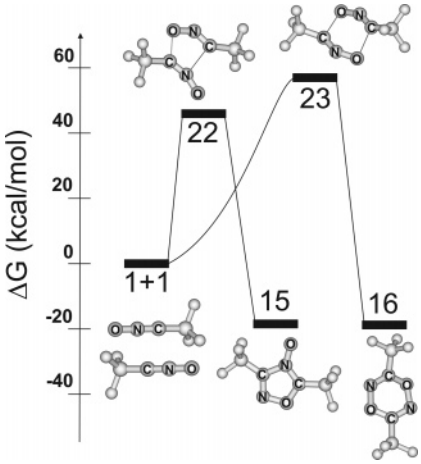

Figure 9. Calculated (UB3LYP/6-311+G(2d)) relative free energies (kilocalories per mole) of the minima and TSs in the dimerization pathways leading from **1** to the two non-furoxan dimer species.

been located on the UB3LYP surface, rotating to **18**. They are not included in Figure 8, but these and additional competing pathways have been located in the dimerization mechanisms for the F-, Cl-, Br-, and CH_3-nitrile oxides.[52]

The alternative dimerization route leading to **15** and **16** (Figure 9) could also occur at higher temperatures; indeed, 1,4-dioxa-2,5-diazine (**16**) has been observed in solution under basic conditions.[12] Both **15** and **16** have TSs for dimerization that suggest a concerted charge-controlled mechanism with ΔG barriers of 46.0 and 57.0 kcal/mol, respectively (Table 6).[67] These TSs have extended structures with the NO groups pointing in opposite directions. Although the 1,2,4-oxadiazole-4-oxide dimer (**15**) retains some attributes of the individual CF_3CNO monomers, it clearly has CN and NO bonds much longer than in **1**, suggesting double bond character for the CN bonds and single bond character for the endocyclic NO bond (Figure 10). The cross-linking NC and CO bonds are on the short side for single bonds, with the latter having a bond length midway between a single and double CO bond. With respect to the furoxan structure (**2**) (Figure 4), the CN double bonds are comparable, whereas the endocyclic NO bond in **15** is significantly shorter, implying an increased stability for this dimer. The exocyclic NO bond is longer (1.261 Å) than that in both the nitrile oxide (**1**) and the furoxan (**2**) which can be explained by much less delocalization with neighboring multiple bonds. For the six-membered ring, 1,4-dioxa-2,5-diazine (**16**), the two combining nitrile oxides have identical bond lengths after forming the ring, although the molecule does not have an inversion center because it is nonplanar. The linking CO bond lengths are between single and double bonds, whereas the NO bonds are long, only slightly shorter than in the long endocyclic bond in **2**. This suggests that at elevated temperatures a dissociation route for **16** could be via a **6**-like structure, which would rapidly lead to either isocyanate (**3**) or cyanate (**4**).

The calculations suggest that the furoxan (**2**) is thermodynamically less stable than the two other minima, **15** and **16**, which have almost the same thermodynamic stability. However, the TSs to **15** (TS **22**) and **16** (TS **23**) are much higher in energy, providing a kinetic stability to the furoxan, the most commonly observed dimerization product.

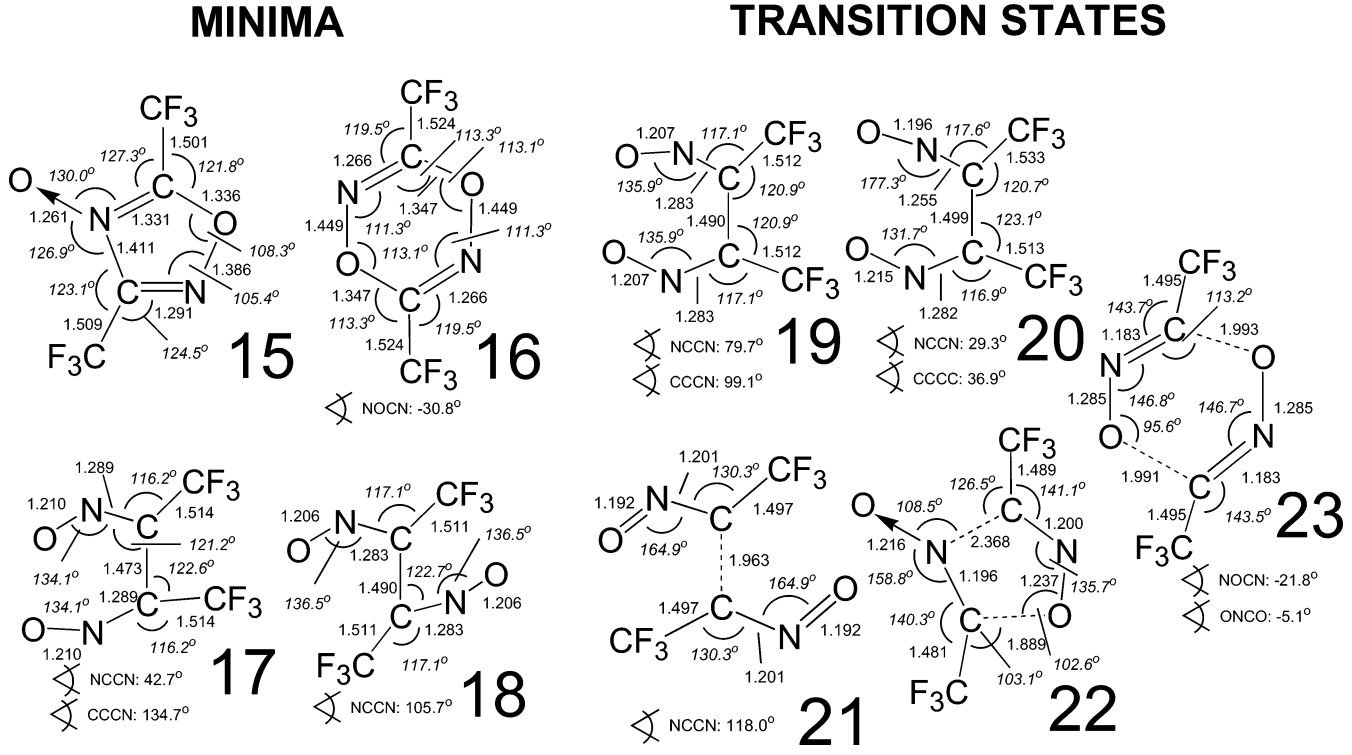

Figure 10. Calculated (UB3LYP/6-311+G(2d)) structures of all minima and TSs in the three dimerization processes.

TABLE 6: Calculated Total and Relative Energies of the $(CF_3CNO)_2$ Isomers and Transition States

struct no.	molecule or TS	total energy (au) UB3LYP/6-311+G(2d)	relative energy[a] UB3LYP/6-311+G(2d)+ZPE (kcal/mol) ΔE	relative energy[a] UB3LYP/6-311+G(2d)+ZPE (kcal/mol) ΔG	$\langle S^2 \rangle$ value
		Minima			
15	1,2,4-oxadiazole-4-oxide	−1011.615 132	−34.8	−18.5[b]	0.0
16	1,4-dioxa-2,5-diazine	−1011.615 042	−35.2	−18.8	0.0
2	furoxan	−1011.605 368	−28.8	−12.4	0.0
17	*ccc*-dinitrosoalkene	−1011.574 837	−11.3	4.8	1.02
18	*ctc*-dinitrosoalkene	−1011.573 735	−10.7	4.3	0.98
		Transition States			
19	**17 ↔ 18**	−1011.573 166	−10.4	5.3	0.99
20	**2 ↔ 17**	−1011.558 822	−2.0	13.9	0.94
21	**1+1 ↔ 18**	−1011.537 093	10.7	25.0	0.13
22	**1+1 ↔ 15**	−1011.503 084	32.3	46.0	0.0
23	**1+1 ↔ 16**	−1011.487 190	41.8	57.0	0.0

[a] Energy relative to that of the sum of the energies of two CF_3CNO monomers. [b] Relative Gibbs free energies (ΔG) at 298.15 K and 1 atm; ZPE and thermal corrections are calculated at the (U)B3LYP/6-311+G(2d) level.

Conclusion

The CF_3CNO molecule has been generated in the gas phase and identified and investigated by mid-IR spectroscopy. The vibrational spectra suggest, but do not confirm, that this molecule has a linear or close-to-linear CCNO chain. On the other hand, the ab initio calculations (CCSD(T)) with a large one particle basis set (cc-pVTZ) suggest, from the calculated structure and the bending potential, that this molecule has strong quasi-symmetric top behavior. B3LYP calculations with triple split valence basis sets concur with this assessment. Clearly, the CF_3CNO molecule requires a high-resolution IR study to investigate the bands in far more detail, to clarify the assignments in the 1160 cm^{-1} region, to locate the bending modes, and to provide further erudition on the linear−bent question. The ring furoxan molecule, formed by trapping and allowing the monomer to dimerize, was also investigated by gas-phase IR with the experimental spectrum compared to B3LYP frequency calculations. Potential loss processes to other pseudohalide isomers were calculated, supporting the notion that the nitrile oxide can exist in the dilute gas phase, as experimentally observed. A B3LYP computational investigation of the monomer/dimer processes demonstrates that the furoxan is kinetically the most favored product, over a relatively low barrier, although other dimer products are feasible, albeit over higher barriers. In the case of dimerization to the furoxan, a multistep process was calculated via singlet diradical species, whereas the formation of the other dimer species is concerted.

Acknowledgment. T.P. and B.H. thank the Hungarian Scientific Research Fund (OTKA grant T031818) for a research grant. N.P.C.W. thanks the Natural Sciences and Engineering Research Council for Discovery and Equipment grants in support of this work.

References and Notes

(1) Grundmann, Ch.; Grünanger, P. *The Nitrile Oxides: Versatile Tools of Theoretical and Preparative Chemistry*; Springer-Verlag: Berlin, 1971.

(2) Caramella, P.; Grünanger, P. In *1,3-Dipolar Cycloaddition Chemistry*; Padwa, A., Ed.; Wiley-Interscience: New York, 1984; Vol. 1, p 291.

(3) Jäger, V.; Colinas, P. A. In *Synthetic Applications of 1,3-Dipolar Cycloaddition Chemistry Toward Heterocycles and Natural Products*; Padwa A., Pearson, W. H., Eds.; Chemistry of Heterocyclic Compounds Series 59; Wiley: New York, 2003; p 361.

(4) Torssell, K. B. G. In *Nitrile Oxides, Nitrones, and Nitronates in Organic Synthesis*; Feuer, H., Ed.; Organic Nitro Chemistry Series; VCH Publishers: New York, 1988.

(5) Kotyatkina, A. I.; Zhabinsky, V. N.; Khripach, V. A. *Russ. Chem. Rev.* **2001**, *70*, 641.

(6) Del'tsova, D. P.; Ananyan, Gambaryan, N. P. *Izv. Akad. Nauk, Ser. Khim.* **1971**, 362.

(7) Truskanova, T. D.; Vasil'ev, N. V.; Gontar, A. F.; Kolomiets, A. F.; Sokol'skii, G. A. *Khim. Geterotsikl. Soedin.* **1989**, *7*, 972.

(8) Tanaka, K.; Masuda, H.; Mitsuhashi, K. *Bull. Chem. Soc. Jpn.* **1984**, *578*, 2184.

(9) Tanaka, K.; Masuda, H.; Mitsuhashi, K.; *Bull. Chem. Soc. Jpn.* **1985**, *587*, 2061. Tanaka, K.; Suzuki, T.; Maeno, S.; Mitsuhashi, K. *J. Heterocycl. Chem.* **1986**, *23*, 1535. Tanaka, K.; Kishida, M.; Maeno, S.; Mitsuhashi, K. *Bull. Chem. Soc. Jpn.* **1986**, *59*, 2631. Tanaka, K.; Masuda, H.; Mitsuhashi, K.; *Bull. Chem. Soc. Jpn.* **1986**, *59*, 3901. Mitsuhashi, K.; Tanaka, K.; Fukuda, J.; Hirose, T. *Seikei Daigaku Kogakubu Kogaku Hokoku* **1987**, *44*, 2983. Mitsuhashi, K.; Tanaka, K. *Kenkyu Hokoku−Asahi Garasu Kogyo Gijutsu Shoreikai* **1988**, *51*, 139.

(10) El Messaoudi, M.; Hasnaoui, A.; Lavergne, J.-P. *Synth. Commun.* **1994**, *244*, 513. Hasnaoui, A.; Baouid, A.; Lavergne, J. P. *J. Heterocycl. Chem.* **1991**, *28*, 73.

(11) Kim, J. N.; Ryu, E. K. *Heterocycles* **1990**, *31*, 633.

(12) Middleton, W. J. *J. Org. Chem.* **1984**, *49*, 919.

(13) Caldwell, C. G.; Chiang, Y.-C.; Dorn, C.; Finke, P.; Hale, J.; Maccoss, M.; Mills, S.; Robichaud, A. (Merck and Co.) U.S. Patent 5877191, March 2, 1999, 98 pp. Caldwell, C. G.; Chiang, Y.-C.; Dorn, C.; Finke, P.; Hale, J.; Maccoss, M.; Mills, S.; Robichaud, A. (Merck and Co.) Patent WO9817660, April 30, 1998, 303 pp.

(14) Nakatani, M.; Ito, M.; Kimijima, K.; Miyazaki, M.; Ueno, R.; Fujinami, M.; Takahashi, S. (Kumiai Chemical Industry Co. Ltd.) Patent WO03010165, February 6, 2003, 78 pp. Bayer, H.; Gewehr, M.; Grote, T.; Mueller, B.; Sauter, H.; Grammenos, W.; Gypser, A.; Ptock, A.; Goetz, R.; Rack, M.; Ammermann, E.; Harries, V.; Lorenz, G.; Strathmann, S.; Roehl, F. (BASF AG) Patent WO9920615, April 29, 1999, 96 pp. Babin, D.; Benoit, M.; Demoute, J. P. (Roussel Uclaf) Patent WO9316054, October 19, 1993, 40 pp.

(15) Pasinszki, T.; Westwood, N. P. C. *J. Phys. Chem.* **1995**, *99*, 6401.

(16) Lichau, H.; Gillies, C. W.; Gillies, J. Z.; Ross, S. C.; Winnewisser, B. P.; Winnewisser, M. *J. Phys. Chem. A* **2001**, *105*, 10065.

(17) Pasinszki, T.; Westwood, N. P. C. *J. Phys. Chem. A* **1996**, *100*, 16856.

(18) Lichau, H.; Ross, S. C.; Lock, M.; Albert, S.; Winnewisser, B. P.; Winnewisser, M.; De Lucia, F. C. *J. Phys. Chem. A* **2001**, *105*, 10080.

(19) Pasinszki, T.; Westwood, N. P. C. *J. Phys. Chem. A* **1998**, *102*, 4939.

(20) Pasinszki, T.; Westwood, N. P. C. *Phys. Chem. Chem. Phys.* **2002**, *4*, 4298.

(21) Koput, J. *J. Phys. Chem. A* **2002**, *106*, 12064.

(22) Pasinszki, T.; Westwood, N. P. C. *J. Phys. Chem. A* **2001**, *105*, 1244.

(23) Kurdyukov, A. I.; Pavlov, V. A.; Gorin, B. I.; Moskva, V. V. *Zh. Obshch. Khim.* **1994**, *64*, 1388.

(24) Glidewell, C.; Holden, H. D. *THEOCHEM* **1982**, *6*, 325.

(25) Kissinger, L. W.; McQuistion, W. E.; Schwartz, M.; Goodman, L. *Tetrahedron* **1963**, *19* (Suppl. 1), 131.

(26) Ungnade, H. E.; Longhran, E. D. *J. Heterocycl. Chem.* **1964**, *1*, 61.

(27) Sheremetev, A. B.; Makhova, N. N.; Friedrichsen. W. *Adv. Heterocycl. Chem.* **2001**, *78*, 66.

(28) Hwang, K.-J.; Jo, I.; Shin, Y. A.; Yoo, S.; Lee, J. H. *Tetrahedron Lett.* **1995**, *36*, 3337. Ferioli, R.; Folco, G. C.; Ferretti, C.; Gasco, A. M.; Medana, C.; Fruttero, R.; Civelli, M.; Gasco, A.. *Brit. J. Pharmacol.* **1995**, *114*, 816. Sorba, G.; Medana, C.; Fruttero, R.; Cena, C.; Di Stilo, A.; Galli, U.; Gasco, A. *J. Med. Chem.* **1997**, *40*, 463. Mu, L.; Feng, S. S.; Go, M. L. *Chem. Pharm. Bull.* **2000**, *48*, 808. Boschi, D.; Tron, G. C.; Di Stilo, A.; Fruttero, R.; Gasco, A.; Poggessi, E.; Motta, G.; Leonardi, A. *J. Med. Chem.* **2003**, *46*, 3762.

(29) Whitney, R. A.; Nicholas, E. S. *Tetrahedron Lett.* **1981**, *22*, 3371. Curran, D. P.; Fenk, C. J. *J. Am. Chem. Soc.* **1985**, *107*, 6023.

(30) Mitchell, W. R.; Paton R. M. *Tetrahedron Lett.* **1979**, *26*, 2443.

(31) Gumanov, L. L.; Korsunskii, B. L. *Izv. Akad. Nauk, Ser. Khim.* **1991**, 1916.

(32) Pulay, P.; Torok, F. *Acta Chim. Hung.* **1965**, *44*, 287. Keresztury, G.; Jalsovszky, G. *J. Mol. Struct.* **1971**, *10*, 304. Pongor, G. Program Scale 3, Department of Theoretical Chemistry, Eotvos Lorand University, Budapest, Hungary, 1993.

(33) Frisch, M. J.; Trucks, G. W.; Schlegel, H. B.; Scuseria, G. E.; Robb, M. A.; Cheeseman, J. R.; Zakrzewski, V. G.; Montgomery, J. A., Jr.; Stratmann, R. E.; Burant, J. C.; Dapprich, S.; Millam, J. M.; Daniels, A. D.; Kudin, K. N.; Strain, M. C.; Farkas, O.; Tomasi, J.; Barone, V.; Cossi, M.; Cammi, R.; Mennucci, B.; Pomelli, C.; Adamo, C.; Clifford, S.; Ochterski, J.; Petersson, G. A.; Ayala, P. Y.; Cui, Q.; Morokuma, K.; Malick, D. K.; Rabuck, A. D.; Raghavachari, K.; Foresman, J. B.; Cioslowski, J.; Ortiz, J. V.; Stefanov, B. B.; Liu, G.; Liashenko, A.; Piskorz, P.; Komaromi, I.; Gomperts, R.; Martin, R. L.; Fox, D. J.; Keith, T.; Al-Laham, M. A.; Peng, C. Y.; Nanayakkara, A.; Gonzalez, C.; Challacombe, M.; Gill, P. M. W.; Johnson, B. G.; Chen, W.; Wong, M. W.; Andres, J. L.; Head-Gordon, M.; Replogle, E. S.; Pople, J. A. *Gaussian 98*, revision A.9; Gaussian, Inc.: Pittsburgh, PA, 1998.

(34) Birkenbach, L.; Sennewald, K. *Justus Liebigs Ann. Chem.* **1931**, *489*, 7.

(35) Edgell, W. F.; Potter, R. M. *J. Chem. Phys.* **1956**, *24*, 80. Alfonzo, P. N.; Anacona, J. R. *J. Chem. Soc., Faraday Trans.* **1992**, *88*, 3397.

(36) Jones, E. A.; Kirby-Smith, J. S.; Woltz, J. H.; Nielsen, A. H. *J. Chem. Phys.* **1931**, *19*, 242.

(37) Koput, J. *J. Phys. Chem. A* **1999**, *103*, 2170.

(38) Koput, J. *J. Phys. Chem. A* **1999**, *103*, 6017.

(39) Koput, J. *J. Phys. Chem. A* **2001**, *105*, 11347.

(40) Csonka, G. I.; Réffy, J. *Chem. Phys. Lett.* **1994**, *229*, 191.

(41) Cremer, D.; Kraka, E.; He, Y. *J. Mol. Struct.* **2001**, *567*, 275.

(42) Bodenseh, H. K.; Morgenstern, K. *Z. Naturforsch.* **1970**, *25a*, 150. Blackburn, P. B.; Brown, R. D.; Burden, F. R.; Crofts, J. G.; Gillard, I. R. *Chem. Phys. Lett.* **1970**, *7*, 102.

(43) He, Y.; Gräfenstein, J.; Kraka, E.; Cremer, D. *Mol. Phys.* **2000**, *98*, 1639.

(44) Cremer, D. *Mol. Phys.* **2001**, *99*, 1899.

(45) Faniran, J. A.; Shurvell, H. F. *Spectrochim. Acta* **1970**, *26A*, 1459.

(46) Faniran, J. A.; Shurvell, H. F. *Spectrochim. Acta* **1971**, *27A*, 1945.

(47) Anacona, J. R.; Alfonzo, P. N. *J. Mol. Struct.*. **1993**, *287*, 111.

(48) Stevens, J.; Schweizer, M.; Rauhut, G. *J. Am. Chem. Soc.* **2001**, *123*, 7326.

(49) Rauhut, G. *Adv. Heterocycl. Chem.* **2001**, *81*, 1.

(50) Figgen, D.; Metz, B.; Stoll, H.; Rauhut, G. *J. Phys. Chem. A* **2002**, *106*, 6810.

(51) Rauhut, G.; Werner, H.-J. *Phys. Chem. Chem. Phys.* **2003**, *5*, 2001.

(52) Havasi, B.; Pasinszki, T.; Westwood, N. P. C. Manuscript in preparation.

(53) Boyer, N. E.; Czerniak, G. M.; Gutowsky, H. S.; Snyder, H. R. J. *J. Am. Chem. Soc.* **1955**, *77*, 4238.

(54) Boyer, J. H.; Toggweiler, U.; Stoner, G. A. *J. Am. Chem. Soc.* **1957**, *79*, 1748.

(55) Kropf, H.; Lambeck, R. *Justus Liebigs Ann. Chem.* **1966**, *700*, 18.

(56) Ungnade, H. E.; Kissinger, L. W. *Tetrahedron* **1963**, *19* (Suppl. 1), 143.

(57) Pasinszki, T.; Ferguson, G.; Westwood, N. P. C. *J. Chem. Soc., Perkin Trans. 2* **1996**, 179.

(58) Durig, J. R.; Guirgis, G. A.; Eltayeb, S. *J. Mol. Struct.* **1994**, *324*, 93.

(59) Steger, B. Ph.D. Thesis, University of Tübingen, 1986. Koput, J.; Stahl, W.; Heineking, N.; Pawelke, G.; Steger, B.; Christen, D. *J. Mol. Spectrosc.* **1994**, *168*, 323.

(60) Kono, M.; Matsumi, Y. *Phys. Chem. Chem. Phys.* **2000**, *2*, 5578.

(61) Houk, K. N.; Yamaguchi, K. In *1,3-Dipolar Cycloaddition Chemistry*; Padwa, A., Ed.; Wiley-Interscience: New York, 1984; Vol. 2, p 407. Houk, K. N.; Gonzalez, J.; Li, Y. *Acc. Chem. Res.* **1995**, *28*, 81.

(62) Huisgen, R. *Angew. Chem., Int. Ed. Engl.* **1963**, *2*, 565; *J. Org. Chem.* **1968**, *33*, 2291; **1976**, *41*, 403. Huisgen, R. In *1,3-Dipolar Cycloaddition Chemistry*; Padwa, A., Ed.; Wiley-Interscience: New York, 1984; Vol. 1, p 1.

(63) Firestone, R. A. *J. Org. Chem.* **1968**, *33*, 2285; **1972**, *37*, 2181; *J. Chem. Soc. A* **1970**, 1570; *Tetrahedron* **1977**, *33*, 3009.

(64) Himmel, H.-J.; Konrad, S.; Friedrichsen, W.; Rauhut, G. *J. Phys. Chem. A* **2003**, *107*, 6731.

(65) Yu, Z.-X.; Caramella, P.; Houk, K. N. *J. Am. Chem. Soc.* **2003**, *125*, 15420.

(66) Pasinszki, T.; Havasi, B. *Phys. Chem. Chem. Phys.* **2003**, *5*, 259.

(67) The ΔG barrier for the formation of **15** is some 9 kcal/mol higher than the similar pathway calculated for CH_3CNO dimerization to the 1,2,4-oxadiazole-4-oxide structure in ref 65.